doi.org/10.36721/PJPS.2025.38.4.REG.13101.1

Periplocin has anti-tumor actions in prostate cancer through modulating the miR-3614-5p/SLC4A4 axis

Jinjun Tian* and Dingguo Zhang
Department of Urology, Shanghai Pudong New Area People's Hospital, Chuanhuan South Road, Pudong New Area, Shanghai, China

Abstract: Periplocin (PPLN) can inhibit malignant tumors including prostate cancer (PC), but its impact on prostate cancer is unknown. Prostate cancer cells were treated with various doses of periplocin (PPLN), and the optimal treatment concentration of PPLN was determined using a CCK-8 assay. Bioinformatics analysis was performed to examine the link between miR-3614-5p and SLC4A4. The influences of miR-3614-5p and SLC4A4 levels on prostate cancer cells were analyzed using CCK-8, EdU, cell-scratch, Transwell, and flow cytometry analyses. A nude-mouse tumor model was created by injecting mice with PC3 cells subcutaneously. MiR-3614-5p and SLC4A4 levels in cancer cells and tumor tissues were measured using quantitative real-time reverse transcription polymerase chain reaction (qRT-PCR) and western blot analyses. 100 nM PPLN dramatically decreased the proliferation, migration, and invasion of prostate cancer cells and promoted apoptosis. MiR-3614-5p reduced SLC4A4 levels, and both the reduction of miR-3614-5p and increase of SLC4A4 expression greatly promoted the malignancy behavior of cells. Low miR-3614-5p expression decreased PPLN's inhibitory effect on malignant behavior, which was reversed by down-regulation of SLC4A4. PPLN reduced tumor growth in mice, increased miR-3614-5p levels, and decreased SLC4A4 levels. In conclusion, PPLN exerted anti-prostate-cancer effects by modulating the miR-3614-5p/SLC4A4 axis.

Keywords: Prostate cancer, periplocin, miR-3614-5p, SLC4A4, malignant biological behavior

Submitted on 11-07-2024 – Revised on 19-11-2024 – Accepted on 09-12-2024

INTRODUCTION

Prostate cancer (PC) is the most prevalent malignant tumor of the male reproductive system and has major consequences for men's health and quality of life. According to data from GLOBOCAN 2020, prostate cancer has the second highest incidence rate of malignancies and the fifth highest mortality rate among men globally (Sung *et al*., 2021). The incidence of prostate cancer has significantly risen and increased with age in China, which is related to social and economic development, lifestyle changes, an aging population, and the continuous improvement of diagnosis, making this cancer the most common among genitourinary types (Liu *et al*., 2022a). There were around 125,646 new cases of prostate cancer in China in 2022, along with 56,239 deaths, and the number is steadily increasing (Xia *et al*., 2022).

In the early stages of prostate cancer, there are no visible clinical symptoms, but as the disease progresses, tumor cells invade and metastasize. Diagnosis is frequently made in the middle or late stages, leading to difficulties with curative therapy and poor prognoses (Gandaglia *et al*., 2015; Guccini *et al*., 2021; Wang *et al*., 2018). Endocrine therapy and chemotherapy are currently the most often used clinical treatments for prostate cancer. However, both endocrine and chemotherapeutic medications have a number of side effects, including reducing patient immunity and causing immunological tolerance, which affect patients' quality of life and the progression of disease improvement (Lacouture *et al*., 2022; Markowski and Carducci, 2017).

Natural products have a wide range of molecular components (Sharma *et al*., 2025), which are being used to develop treatments for prostate cancer or to delay metastasis or progression. Periplocin (PPLN) is the main monomer that is extracted from the dried root bark of *Periplocca sepium Bge.* PPLN is considered to have diuretic and decongestive properties, expel "wind-dampness," strengthen the muscles and bones, and have antitussive and cardiotonic properties (Hao *et al*., 2023; Li *et al*., 2016). Investigations have shown that PPLN inhibits the proliferation capacity of a variety of malignant tumor cell lines and promotes apoptosis. Wang *et al*. (2023) discovered that PPLN suppresses the growth of colorectal cancer cells by binding to and inhibiting Lys210 ubiquitination and degradation of LGALS3 (galectin 3), resulting in increased lysosomal autophagy and aggravating lysosomal damage. Lin *et al*. (2023) found that PPLN suppresses the proliferation of hepatocellular carcinoma cells *in vivo* and *in vitro* by disrupting the AKT/NF-κB signaling pathway and decreasing myeloid-derived suppressor cells.

PPLN causes the apoptosis of pancreatic cancer cells by activating the AMPK/mTOR pathway, attenuates cell migration and invasion, and inhibits the growth of pancreatic cancer in nude mice (Xie *et al*., 2021). Furthermore, PPLN restores the responsiveness of pancreatic cancer cells to medication (gemcitabine) by

**Corresponding author:* e-mail: tianjinjun@shpdph.com

blocking the Nrf2-mediated pathway (Bae *et al*., 2023). These findings indicate that PPLN could function as in inducer and sensitizer of tumor-cell apoptosis. It has been demonstrated that PPLN can suppress the activity of prostate cancer cells and promote apoptosis (Bloise *et al*., 2009). However, the molecular mechanism of PPLN in prostate cancer cells has not been sufficiently investigated. Exploring the regulatory mechanisms of PPLN on the malignant biological activity and tumor growth of prostate cancer cells could assist in creating novel medications for prostate cancer and improve treatment approaches.

MicroRNA (miRNA) is a type of endogenous RNA with a length of around 19–24 nucleotides that plays an import part in the formation of several human malignant tumors, including prostate cancer (Hussen *et al*., 2021). In comparison to normal cells, prostate cancer cells have a large amount of dysregulated miRNA that affects tumor-cell metabolism, apoptosis, invasion, and metastasis, which occurs through the silencing tumor-suppressor genes or activation of pro-oncogenic pathways (Khanmi *et al*., 2015). MiR-3614-5p is 24 nt long and is situated on chromosome 17q22 (Han *et al*., 2021). This miRNA has been shown to be significantly under-expressed in various types of cancer, such as breast cancer (Wang *et al*., 2019), lung adenocarcinoma (Shang *et al*., 2019), hepatocellular carcinoma (Feng *et al*., 2021), colorectal cancer (Han *et al*., 2021), non-small-cell carcinoma (Li *et al*., 2020), and prostate cancer (Hsieh *et al*., 2022).

Up-regulating the expression level of miR-3614-5p can effectively inhibit the development of malignancy by these tumor cells. Furthermore, its expression level was found to be connected with the prognosis of cancer (Han *et al*., 2021), suggesting that it could be used as a therapeutic target in prostate cancer. However, the levels of miR-3614-5p associated with prostate cancer and the related regulatory mechanisms involved are currently unknown.

This study examined whether PPLN regulates the proliferation, migration, invasion, and death of prostate cancer cells. MiR-3614-5p and its target genes were explored in regard to the effects of PPLN on the malignant behaviors of prostate cancer cells and tumor growth. The findings could help to elucidate how PPLN impacts prostate cancer and provide new insights for diagnosis and treatment.

MATERIALS AND METHODS

Drugs and reagents

PPLN (HY-N1381, 99.92% purity), CCK-8 reagent (HY-K0301), and antifade mounting medium (HY-K1042) were purchased from Med Chem Express (Monmouth Junction, NJ, USA). Fetal bovine serum (FBS, C0235), paraformaldehyde (P0099), crystal violet (C0121), a dual luciferase reporter gene assay kit (RG027), DAB solution (P0203), hematoxylin (C0107), ECL (P0018S), and neutral resin (C0173) were purchased from Beyotime (Shanghai, China). RPMI-1640 medium (ORCPM0110B) was purchased from ORi Cells Biotechnology (Shanghai, China). Lipofectamine 3000 (L3000001) and polyvinylidene fluoride (PVDF) membrane were purchased from Invitrogen (Austin, TX, USA). An EdU cell proliferation detection kit (C10310-1) was purchased from RiboBio (Guangzhou, China).

Triton X-100 (X100), DAPI staining solution (D9542), bovine serum albumin (V900933), and sodium dodecyl sulfate-polyacrylamide gel (L4509) were purchased from Sigma-Aldrich (St. Louis, MO, USA). Transwell chambers and Matrigel matrix gel (354230) were purchased from Corning (Tewksbury, MA, USA). An annexin V-FITC/PI apoptosis detection kit (40302ES20) and RIPA lysis buffer (20101ES60) were purchased from Yeasen (Shanghai, China).

Rabbit anti-Ki-67 (ab232784), sheep anti-rabbit IgG (ab150077), anti-SLC4A4 (ab187511), and anti-GAPDH (ab9485) were obtained from Abcam (Waltham, Massachusetts, USA). Trizol reagent (DP424) was obtained from TIANGEN (Beijing, China). A Prime Script RT reagent kit (RR047 A) was obtained from Takara (Tokyo, Japan), and a SYBR Green PCR kit (4309155) was obtained from Applied Biosystems (Delaware, USA). Pierce protein-free containment buffer (37573) was purchased from Thermo Fisher (Waltham, MA, USA).

Bioinformatics examination

The Target Scan (https://www.targetscan.org/vert_80/), GEPIA2 (http://gepia2.cancer-pku.cn/#index) and starBase (https://rnasysu.com/encori/) databases were used to search for possible miR-3614-5p target genes. The screening parameters included adj. $P<0.05$ and Log2 (fold change) ≥ 2. The levels of SLC4A4 in prostate cancer tissues and normal prostate tissues from the TCGA database were examined using GEPIA2 online. The binding sites of miR-3614-5p and SLC4A4 were determined based on the Target Scan database.

Cell cultivation

Normal human prostate epithelial cells (RWPE-1) and prostate cancer cells (DU-145 and PC3) were obtained from the Chinese Academy of Sciences cell bank. Using RPMI-1640 medium with 10% FBS, the cells were incubated at 37°C in an atmosphere containing 5% CO_2 by volume. The medium was changed on the next day to continue incubation. Once the cells reached fusion, they were passaged and amplified.

Cell transfection

RiboBio (Guangzhou, China) supplied the miR-3614-5p mimic/inhibitor (mimic/inhibitor) and its negative control

(mimic-NC and inhibitor-NC), SLC4A4 overexpression vector (SLC4A4) and its negative control (vector), and SLC4A4 low expression vector (si-SLC4A4) and its negative control (si-NC). Transfection was carried out in accordance with the instructions for Lipofectamine 3000. 48 h later, tests were conducted *in vitro* and *in vivo*.

CCK-8 detection

Prostate cancer cells (DU145 and PC3) and RWPE1 cells were digested with trypsin, centrifuged, counted and inoculated into 96-well plates (1×10^4 cells/well). 200 μL of medium containing PPLN (25, 50, 100, 200 and 500 nM) were dispensed into each well, followed by 48 hours of cell culture. Next, 20 μL of CCK-8 reagent solution were introduced into every well and mixed. After reaction for 4 h, the proliferation of cells in each well was determined using a DR-200Bc enzyme labeling device based on the optical density (OD) at 450 nm (Hiwell-Diatek Instruments, Jiangsu, China) .

EdU detection

The proliferation of prostate cancer cells was identified using an EdU cell proliferation detection kit. The cells were cultivated with 100 nM PPLN for 24 h, washed with PBS, and incubated with 10 μM EdU staining reaction solution for 1 h in darkness. After rinsing twice with PBS, the cells were treated with 4% paraformaldehyde for 15 min. For permeabilization, a solution of PBS with 0.3% Triton X-100 was introduced for 10 min, and Click reaction solution was left to incubate for 30 min away from light. DAPI staining solution was then added and incubated for about 10 min. After sealing the film with antifade mounting medium, the cells were examined and photographed using an MF52-N fluorescence microscope (Mshot, Guangzhou, China), and the positively stained cells were assessed.

Scratch-wound assay

DU-145 and PC3 cells were digested with trypsin and resuspended in PBS. Next, 1 mL of cell suspension (5×10^5 cells/well) was aspirated with a sterile pipette tip and inoculated into 6-well plates where horizontal lines had been drawn beforehand. When the cells had completely attached to the walls and grew to more than 80% density, a uniform straight line was drawn perpendicular to the bottom of the well plate with a sterile 200-μL pipette tip.

The suspended cells were removed using PBS, and serum-free cell culture medium containing 100 nM PPLN was added (the control received serum-free medium only). This was followed by incubation for 24 h. Microscopy photographs were taken at 0 h and 24 h, and the scratch widths were calculated using Image J software to quantify the migration rate of each group of cells. The migration rate was calculated as follows: *Migration rate (%) = (0-h scratch width – 24-h scratch width) / 0-h scratch width × 100%.*

Transwell assay

Transwell chambers were placed in 24-well plates, and pre-cooled Matrigel was added to the chambers and air-dried. Cell suspension (cell density: 1×10^5/mL, 100 μL) was then added to the upper chamber, followed by the addition of complete medium containing 100 nM PPLN in the lower chamber. The plates were incubated at 37°C in 5% CO_2 for 24 h. The migrating cells on the lower surface were exposed to 4% paraformaldehyde before being dyed using 0.1% crystal violet. High-magnification microscopy was used to observe and photograph the quantities of cells that invaded the lower compartment.

Flow cytometry

DU-145 and PC3 cells were tested for apoptosis with the annexin V-FITC/PI apoptosis detection kit. Cells were treated with 100 nM PPLN for 24 h, digested, collected, rinsed with PBS, and gently mixed with 100 μL of binding buffer. Annexin V-FITC and propidium iodide (PI) were then introduced, followed by incubation for 10 min in a dark environment. Each sample was treated with 400 μL of binding buffer and analyzed with a BD FACSCelesta™ flow cytometer (BD, NJ, USA) within 1 hour.

Dual-luciferase reporter assay

The dual luciferase reporter plasmids for wild-type (WT) and mutant (MUT) SLC4A4 3′UTR were obtained from RiboBio Co., Ltd. The two plasmids were co-transfected with miR-3614-5p mimic and mimic-NC, respectively, into prostate cancer cells using Lipofectamine 3000. Following a 48-h transfection period, each set of cells was collected, and the luciferase activity of the transfected cells was determined using the instructions of the dual-luciferase reporter gene assay kit.

In vivo experiments

20 BALB/c male nude mice were obtained from the Laboratory Animal Center of the Chinese Academy of Sciences (Shanghai, China). To create a tumor model, each mouse received a subcutaneous injection of 100 μL of PC3 cell solution (5×10^7 cells/mL) in the right axilla. When the tumor volume reached 150 mm^3 (Zhou *et al*., 2020), the mice were randomly assigned to a control group (Ctrl) and a PPLN group.

The PPLN group was intraperitoneally given 20 mg/kg PPLN (diluted in saline) every other day for a total of 7 times. The Ctrl group was treated with an equal volume of saline only. Every 7 days, the tumor volume (1/2 × length × $width^2$) was measured using vernier calipers and photographed. After the injection of medication, the mice were kept until the 28th day and then sacrificed, and the tumors were isolated and weighed. This study was approved by Shanghai Pudong New Area People's Hospital (No. KY20231907).

Immunohistochemistry

After fixation with 4% paraformaldehyde for 24 h, tumor

tissues were deparaffinized and hydrated in paraffin sections, and antigen repair was performed using a microwave oven. Endogenous peroxidase was inactivated with 3% H_2O_2, and then the tissues were evenly covered with drops of 5% bovine serum albumin and closed for 30 min. Following that, rabbit anti-Ki-67 (1:100) was added dropwise, followed by incubation at 4ºC overnight. The tissues were then washed with PBS to remove the floating color, covered with streptavidin-horseradish peroxidase complex-labeled sheep anti-rabbit IgG (1:1000), and kept at 37ºC for 1 h.

Following incubation, the sample was washed again with PBS. The color was developed for 10 min using DAB solution, followed by 5 min of restaining with hematoxylin. Sections were sealed with neutral resin, and the quantity of positively brown-stained cells was viewed using a microscope.

Quantitative real-time reverse transcription polymerase chain reaction (qRT-PCR) assay

Total RNA was extracted by lysing tissue samples and different cells with Trizol reagent. The RNA was reverse transcribed into cDNA using a Prime Script RT reagent kit. The target gene was amplified using a SYBR Green PCR kit, and PCR was carried out using an ABI PRISM 7300 RT-PCR system (7300, ABI, Carlsbad, CA, USA). Data were analyzed using the $^{-\Delta\Delta Ct}$ method. The primers were designed as follows: miR-3614-5p: F: 5'-GGGGAG CCCAGACGGG-3'; R: 5'-AGTGCAGGGTCCGA GGTATT-3'. U6: F: 5'-CCCTTCGGGGACATCCGATA-3'; R: 5'-TTTGTGCGTGTCATCCTTGC-3'.

Western blot analysis

Total proteins from prostate cancer cells and tumor tissues were extracted using RIPA lysis buffer, and their concentrations were calculated. The proteins in the sample were separated through electrophoresis on 10% sodium dodecyl sulfate-polyacrylamide gel and then shifted to a PVDF membrane. After membrane transfer, the membranes were incubated in Pierce protein-free containment buffer for 15 min. The membranes were incubated with anti-SLC4A4 (1:1000) and the internal reference anti-GAPDH (1:1000) at 4°C overnight.

On the following day, the membranes were exposed to secondary antibody (1:2000) for 1 h at room temperature. The membranes were washed with Tris-buffered saline with Tween 20 (TBST) and visualized using ECL. The grayscale values of each protein band were obtained after processing the images using Image J software (National Institutes of Health, Bethesda, MD, USA).

Ethical approval

This study was approved by Shanghai Pudong New Area People's Hospital (No. KY20231907).

STATISTICAL ANALYSIS

A minimum of 3 repetitions were performed for each experiment, and the results are reported the as mean and standard deviation. Statistical analysis was conducted using the software SPSS 26.0 (IBM SPSS Statistics 26). The differences between groups were evaluated using Student's *t*-test and an analysis of variance (ANOVA). $P<0.05$ indicated statistically significant differences. The results were plotted using the software Graphpad Prism 9.0.

RESULTS

PPLN reduces the malignant phenotype and causes apoptosis in PC cells

RWPE1 cells and prostate cancer cells (DU145 and PC3) were treated with PPLN to determine appropriate treatment concentrations. PPLN did not initially have a significant effect on the viability of RWPE1 cells, but a decrease in cell viability occurred when the PPLN concentration was increased to 200nM (fig. 1A). The addition of PPLN to the culture medium had a significant inhibitory impact on the proliferative viability of prostate cancer cells, and the impact gradually increased with the concentration of PPLN. The inhibitory effect was significantly increased when the concentration was greater than 100nM (fig. 1B–1C). As a result, we chose 100nM as the treatment concentration for PPLN in the *in vitro* tests.

The number of EdU-positive cells was dramatically reduced in both DU145 and PC3 cells after 24 h of PPLN treatment (fig. 1D–1E), which demonstrates that PPLN effectively suppressed the proliferation of prostate cancer cells. The scratch-wound assay showed that PPLN had an effect on the migratory ability of the prostate cancer cells. After 24 h, the migration rate of DU145 and PC3 cells treated with 100 nM PPLN notably decreased (fig. 1F–1G).

In the Transwell invasion experiment, 100 nM of PPLN greatly reduced the number of invading DU145 and PC3 cells (fig. 1H–1I). In the flow cytometry experiment, 100 nM PPLN significantly promoted apoptosis in both DU145 and PC3 cells (fig. 1J–1K). All these findings imply that PPLN can inhibit the malignant phenotype and increase apoptosis in tumor cells *in vitro*, but its mechanism of action requires further investigation.

PPLN suppresses the malignant phenotype and increases apoptosis in PC cells via upregulating miR-3614-5p

It has been established that the level of miR-3614-5p is down-regulated in prostate cancer, and its gene has tumor-suppressing effects (Fu *et al*., 2024). Therefore, we evaluated the influence of PPLN on miR-3614-5p production to see whether it mediates miR-3614-5p's

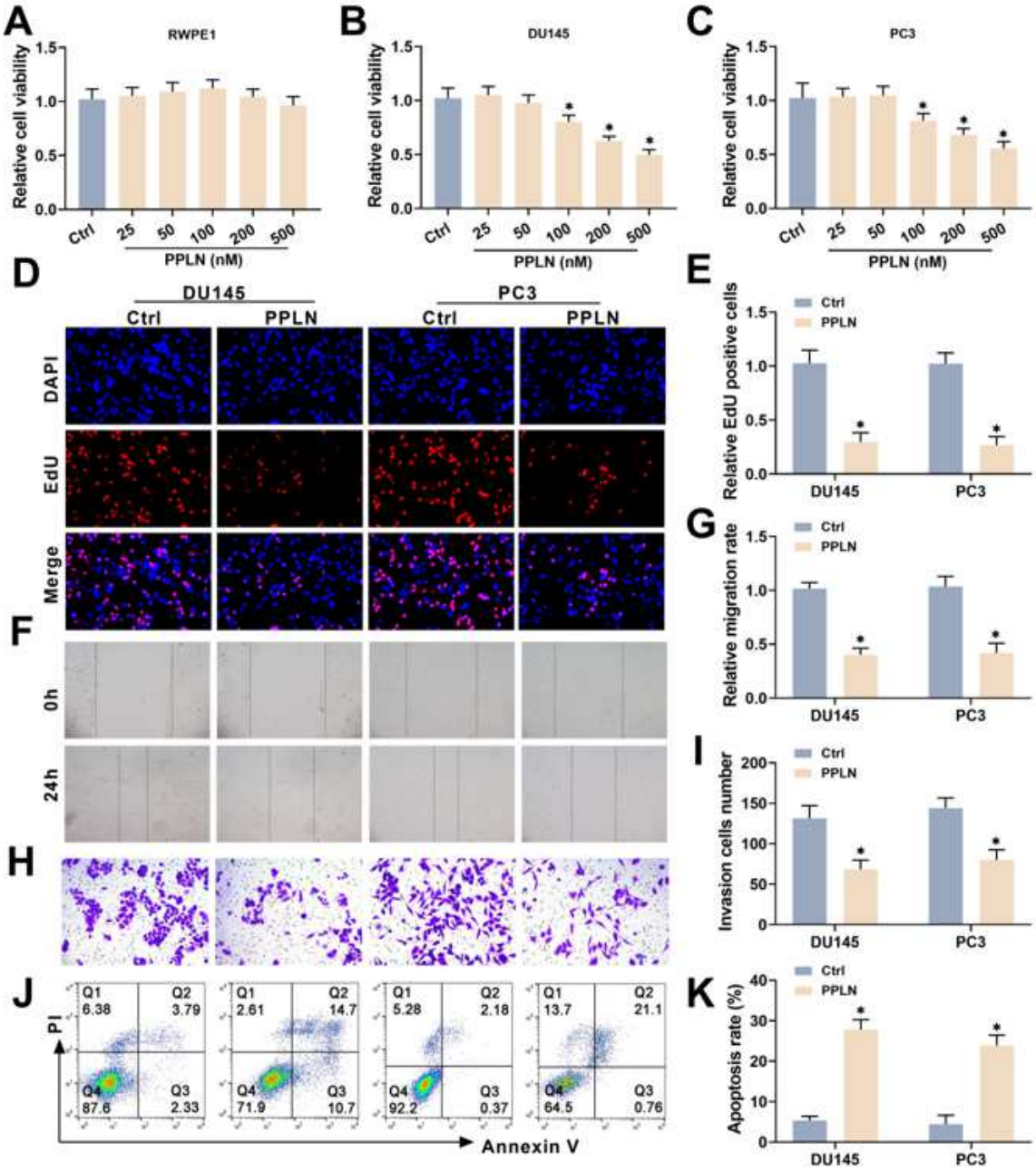

(A–C) CCK-8 detected the inhibitory influence of various concentrations of PPLN on the proliferation of RWPE1 cells and prostate cancer cells (DU145 and PC3). 100 nM of PPLN significantly inhibited the cell viability of prostate cancer cells but had no significant effect on RWPE1 cells. Thus, this concentration was used in the following tests. (D-E) EdU detected the fraction of DU145 and PC3 positive cells, which indicated cell proliferation. (F–G) Scratch-wound assay to determine the migratory capacity of DU145 and PC3 cells. (H–I) Transwell detection of the number of DU145 and PC3 cells infiltrating the lower chamber to assess cell invasion capability. (J–K) A flow test to detect apoptosis in DU145 and PC3 cells. (*P<0.05).

Fig. 1: PPLN inhibited the malignant phenotype and induced apoptosis in prostate cancer cells

suppressive effect on tumor cells. The qRT-PCR results indicated a notable decrease in the level of miR-3614-5p in prostate cancer cells (DU145 and PC3) in comparison to normal human prostate epithelia l cells (RWPE1) (fig. 2A). However, after treatment with 100 nM PPLN, the miR-3614-5p expression levels were considerably elevated in DU145 and PC3 cells (fig. 2B), which suggested that PPLN might reduce tumor-cell malignancy by upregulating miR-3614-5p expression.

Tumor cells were treated with miR-3614-5p inhibitor to support the findings from the previous experiment. The miR-3614-5p inhibitor was transfected into prostate cancer cells, and its inhibitory efficacy was verified using qRT-PCR (fig. 2C). The trials were divided into three groups: a control group (Ctrl), a group treated with 100

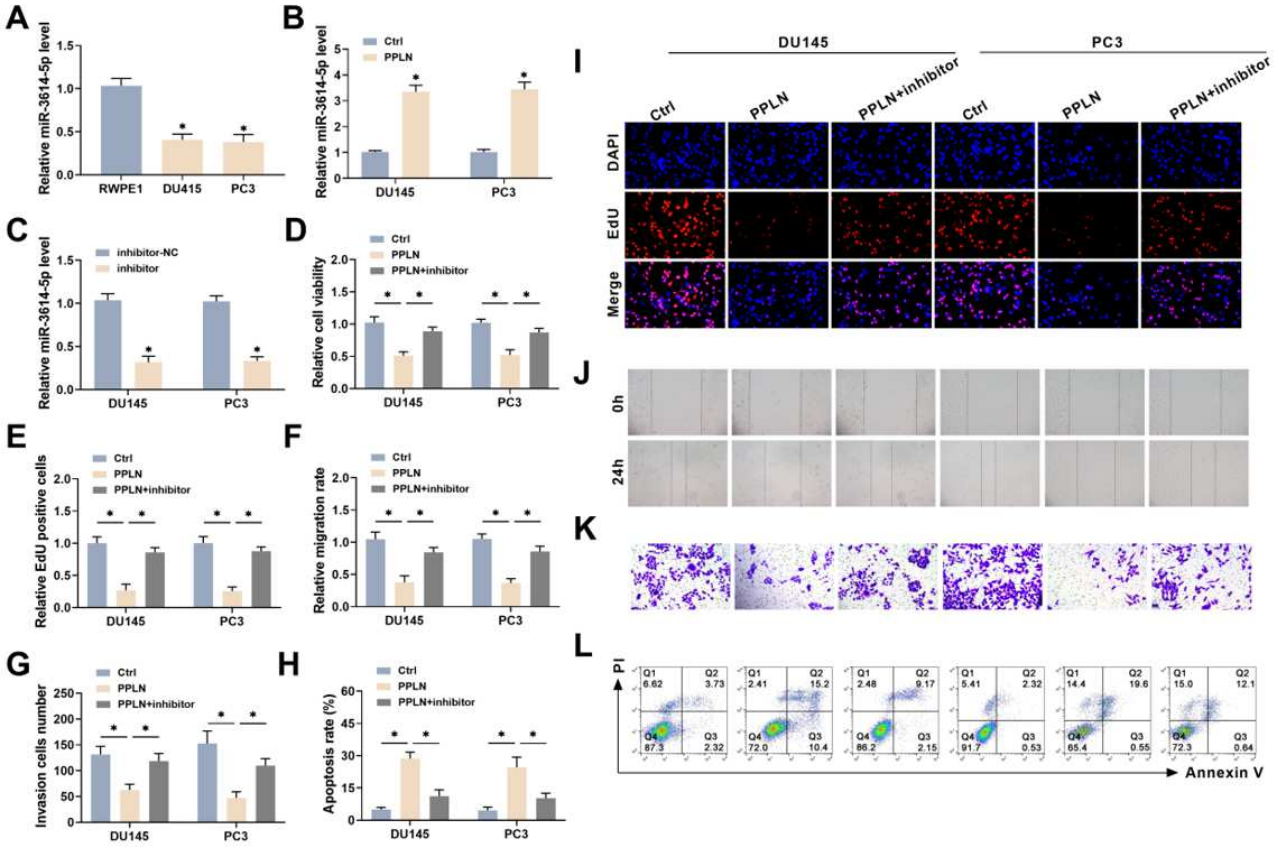

(A) qRT-PCR was used to detect the expression of miR-3614-5p in RWPE1 normal human prostate epithelial cells and prostate cancer cell lines DU145 and PC3. (B) qRT-PCR was used to assess the effect of 100 nM PPLN on miR-3614-5p level in DU145 and PC3 cells. (C) qRT-PCR was used to determine the knockdown effects of miR-3614-5p in DU145 and PC3 cells following transfection with the miR-3614-5p inhibitor. (D) CCK-8 assessed the proliferative viability of DU145 and PC3 cells under various treatment conditions. (E, I) EdU showed a positive ratio of DU145 and PC3 cells under different treatment settings when assessing cell proliferation. (F, J) Scratch-wound assay for detecting DU145 and PC3 cell movement. (G, K) Transwell test to determine the quantity of DU145 and PC3 cells invading the lower chamber and assessing cell invasion ability. (H, L) Flow cytometry was used to detect apoptosis in DU145 and PC3 cells. (**P*<0.05)

Fig. 2: PPLN reduced the malignant phenotype and caused apoptosis in prostate cancer cells by upregulating miR-3614-5p

nM PPLN (PPLN), and a group treated with 100 nM PPLN and transfected with the miR-3614-5p inhibitor (PPLN+miR-3614-5p inhibitor). As shown in fig. 2D–2L, the PPLN group's cell proliferation, migration, and invasion were significantly reduced, and the apoptosis rate was notably increased. However, down-regulation of miR-3614-5p expression partially weakened the effect of PPLN. Rescue tests showed that PPLN suppressed the malignant activity of prostate cancer cells by increasing miR-3614-5p.

PPLN suppresses SLC4A4 expression by upregulating miR-3614-5p

We screened the downstream target gene of miR-3614-5p, *SLC4A4*, using the Target Scan, GEPIA2, and starBase databases (fig. 3A). We then analyzed the expression level of *SLC4A4* in the TCGA database using GEPIA online. The SLC4A4 level was markedly higher in prostate cancer tissues than in normal tissues (fig. 3B). Given the down-regulation of miR-3614-5p level in prostate cancer tissues, it appears that miR-3614-5p may be targeted to suppress SLC4A4.

Using the Target Scan database, we found a target site in miR-3614-5p for binding with SLC4A4 (fig. 3C). For verification, we confirmed the impact of transfection of a mimic of miR-3614-5p (fig. 3D) and then co-transfected *SLC4A4* WT and SLC4A4 MUT plasmids with the miR-3614-5p mimic and mimic-NC into prostate cancer cells using Lipofectamine 3000. As demonstrated in fig. 3E, the miR-3614-5p mimic substantially suppressed *SLC4A4* WT luciferase activity in prostate cancer cells while having no significant effect on *SLC4A4* MUT, indicating that miR-3614-5p targeted and decreased SLC4A4 expression.

Western blot analysis revealed that down-regulation of miR-3614-5p in prostate cancer cells significantly

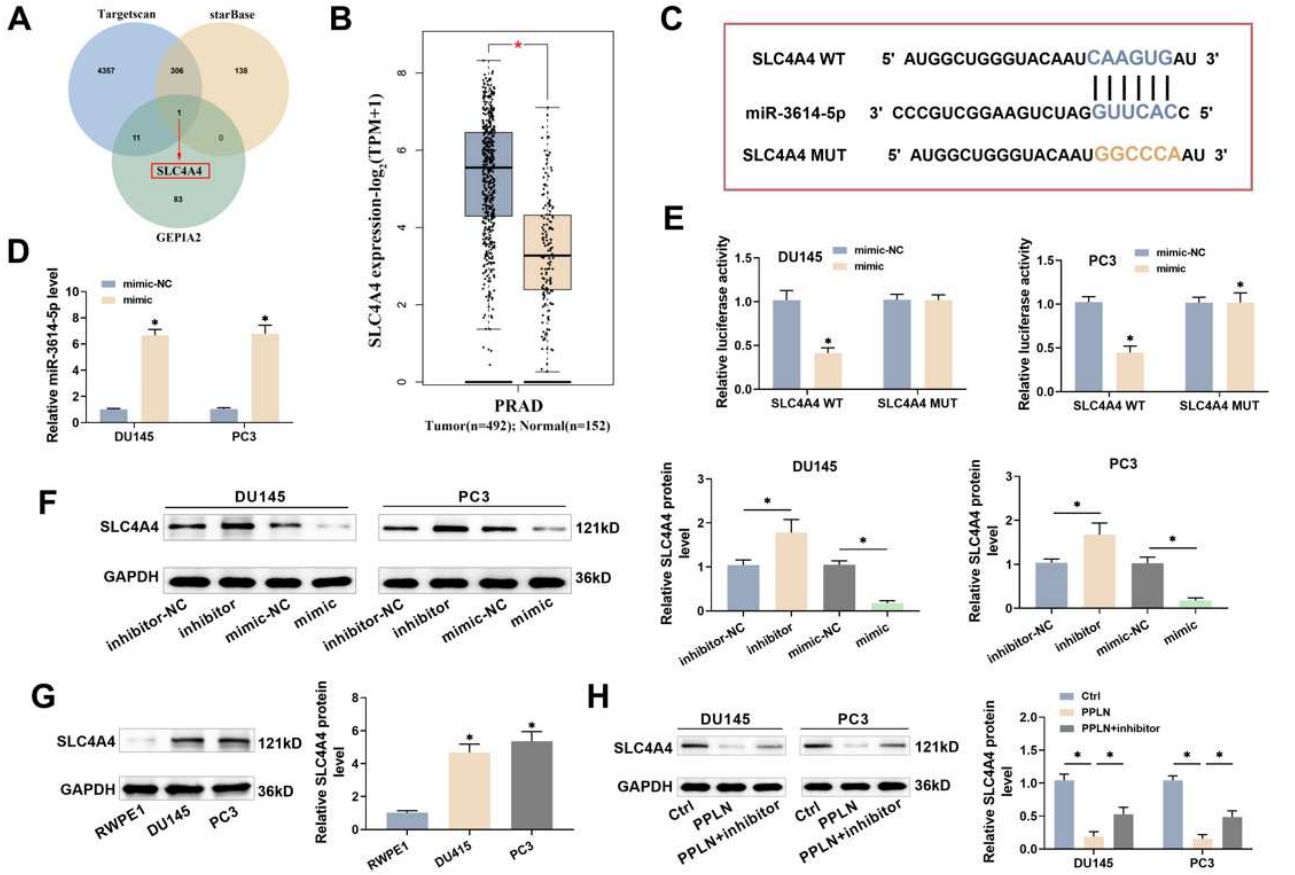

(A) The probable target gene of miR-3614-5p was identified as SLC4A4 using the Target Scan, star Base, and GEPIA2 databases. (B) Using GEPIA, the differential expression of SLC4A4 in 492 prostate cancer tissues and 152 normal prostate tissues from the TCGA database was investigated. (C) The Target Scan database revealed the binding location of miR-3614-5p with SLC4A4. (D) qRT-PCR was used to assess miR-3614-5p overexpression's effects following transfection of miR-3614-5p mimics in DU145 and PC3 cells. (E) A dual-luciferase test was used to confirm the targeting connection between miR-3614-5p and SLC4A4. (F) Western blot analysis of SLC4A4 expression alterations following miR-3614-5p knockdown/over expression in DU145 and PC3 cells. (G) Western blot was used to determine SLC4A4 expression levels in RWPE1 normal human prostate epithelial cells and pre-prostate cancer cell lines DU145 and PC3. (H) Western blot was used to assess the influence of PPLN on SLC4A4 expression in DU145 and PC3 cells. (*P<0.05).

Fig. 3: PPLN suppressed SLC4A4 expression via upregulating miR-3614-5p

promoted SLC4A4 expression and up-regulation inhibited it (fig. 3F). The SLC4A4 level was significantly higher in prostate cancer cells than in RWPE1 cells (fig. 3G). PPLN treatment notably decreased SLC4A4 level in prostate cancer cells, whereas inhibition of miR-3614-5p markedly weakened the influence of PPLN (fig. 3H). Our findings suggest that PPLN targets and inhibits SLC4A4 expression in prostate cancer cells by up-regulating miR-3614-5p.

Increased levels of SLC4A4 inhibits miR-3614-5p's inhibitory influence on the malignant behavior of PC cells

We examined whether miR-3614-5p might target SLC4A4 and alter the malignant progression of prostate cancer cells by transfecting prostate cancer cells into three groups: A control group (Ctrl), one with miR-3614-5p overexpression (mimic), and one with miR-3614-5p overexpression + SLC4A4 overexpression (mimic + SLC4A4). Transfection of the SLC4A4 vector efficiently increased SLC4A4 levels in prostate cancer cells (fig. 4A). The mimic group's cell proliferation, migration, and invasion capacities were dramatically reduced, while the apoptosis rate increased. The mimic + SLC4A4 group had considerably stronger cell proliferation, migration, and invasion capacities and a lower apoptosis rate compared to the mimic group (fig. 4B–4J). As a result, overexpressing SLC4A4 reversed miR-3614-5p's inhibitory effect on prostate cancer cell malignancy.

PPLN reduces prostate cancer cells' malignant behavior via modulating the miR-3614-5p/SLC4A4 axis

We also transfected the si-SLC4A4 vector into prostate cancer cells and verified the effects of its transfection (fig. 5A) to further investigate the impact of low SLC4A4 expression. There were four groups in this experiment: a control group (Ctrl), one with 100 nM PPLN treatment (PPLN), one with 100 nM PPLN treatment and low miR-

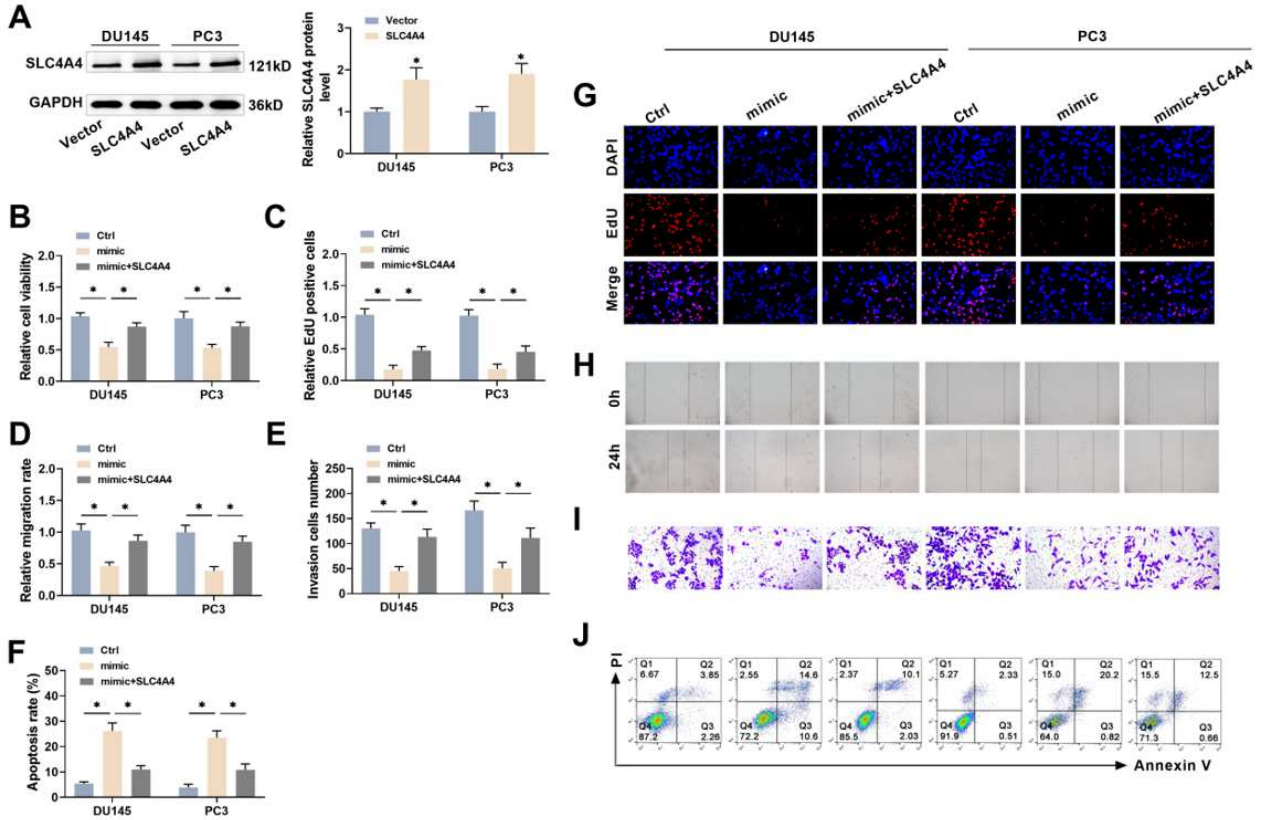

(A) The SLC4A4 expression vector was transfected into prostate cancer cells, and the overexpression effects of SLC4A4 was determined by western blot. (B) CCK-8 detected the proliferative viability of DU145 and PC3 cells under various treatment conditions. (C, G) EdU showed a positive ratio of DU145 and PC3 cells under various treatment settings used to assess cell proliferation. (D, H) Scratch-wound assay for migratory ability of DU145 and PC3 cells. (E, I) The number of DU145 and PC3 cells invading the lower chamber was measured using a transwell test to assess cell invasion ability. (F, J) Flow cytometry was used to detect apoptosis in DU145 and PC3 cells. (**P*<0.05)

Fig. 4: miR-3614-5p overexpression decreased the malignant phenotype and caused death in prostate cancer cells, while SLC4A4 overexpression reversed this effect.

3614-5p expression (PPLN + inhibitor), and one with 100 nM PPLN treatment and low expression of both miR-3614-5p and SLC4A4 (PPLN + mimic + SLC4A4). Consistent with previous assays, down-regulation of miR-3614-5p expression effectively weakened the inhibitory impact of PPLN on the malignant behaviors of prostate cancer cells. Simultaneous transfection with the si-SLC4A4 vector resulted in a notable decrease in the proliferation, migration, invasive ability of prostate cancer cells, and apoptosis rate (fig. 5B-5J). The results indicated that low SLC4A4 low expression can counteract the weakening impact of low miR-3614-5p low expression on PPLN action, which demonstrated that PPLN prevented malignant behavior by mediating the miR-3614-5p/SLC4A4 axis.

PPLN suppresses development of prostate cancer tumor in vivo

In vivo investigations were conducted to determine whether PPLN decreases the tumorigenic potential of subcutaneous cancer cells in nude mice by modulating the miR-3614-5p/SLC4A4 axis. We injected two groups of stably infected PC3 cells subcutaneously into nude mice given with equal doses of saline (control group) and PPLN (20 mg/kg) intraperitoneally (PPLN group). Nude mice were sacrificed on the 28th day after the end of drug administration, when and their tumors were extracted (fig. 6A).

The *in vivo* tumor growth in the PPLN group was slow, and tumors were smaller than those in the Ctrl group (fig. 6B and 6C). Immunohistochemistry showed that Ki67 expression was much lower in the PPLN group than the Ctrl group (fig. 6D), meaning that PPLN effectively limited the growth of prostate cancer cells *in vivo*. Following PPLN administration at 20 mg/kg, the levels of miR-3614-5p in tumor tissues were considerably elevated, and SLC4A4 levels were lower (fig. 6E and 6F). These results show that PPLN decreased tumor growth in nude mice by upregulating miR-3614-5p and inhibiting SLC4A4 expression.

DISCUSSION

The treatment of malignant tumors with traditional Chinese medicine has advantages of multiple pathways

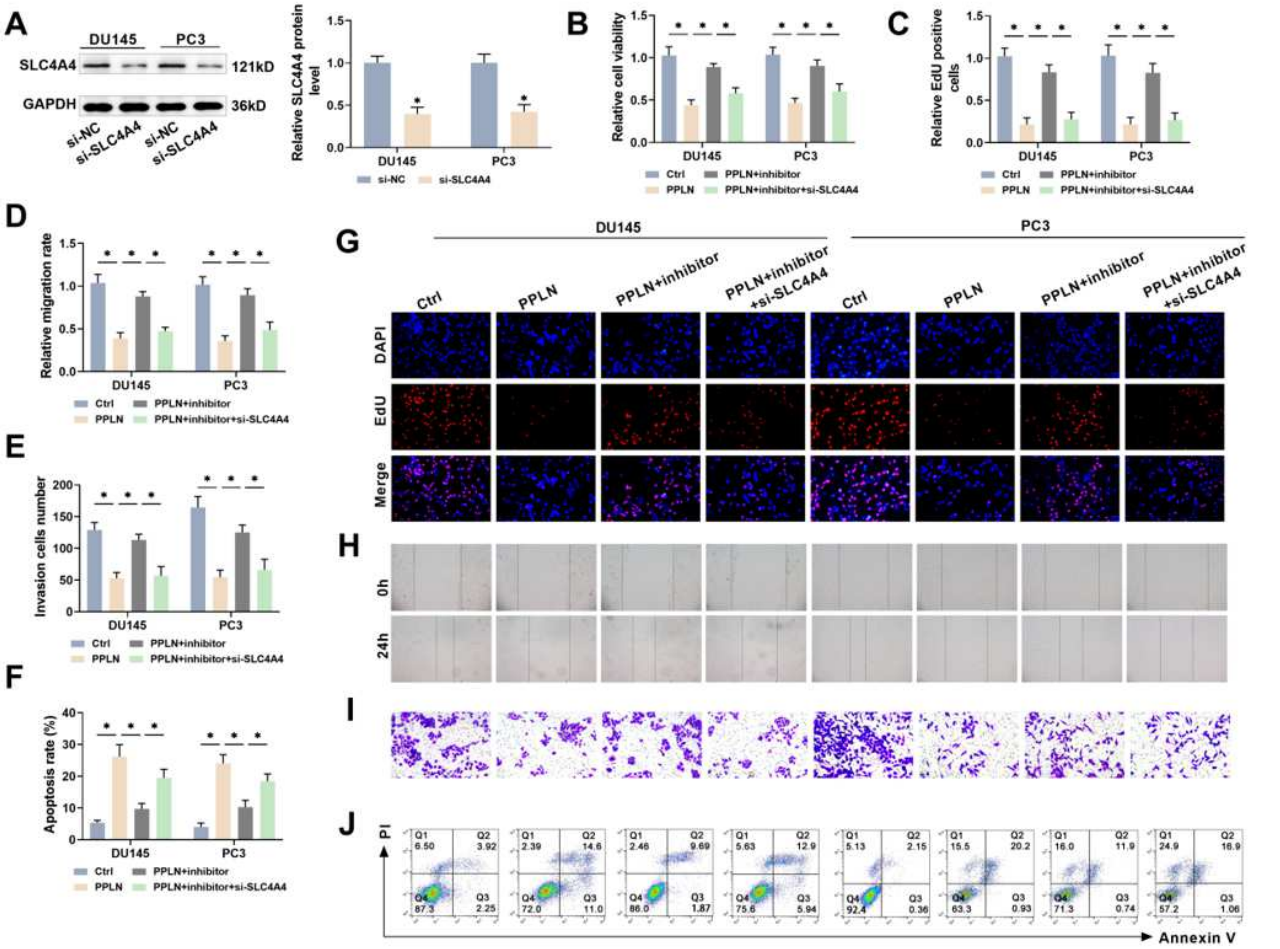

(A) si-SLC4A4 was transfected into DU145 and PC3 cells, and the effects of SLC4A4 knockdown were determined using western blot. (B) CCK-8 assessed the proliferative viability of DU145 and PC3 cells under various treatment conditions. (C, G) EdU showed a positive ratio of DU145 and PC3 cells under various treatment settings to assess cell proliferation. (D, H) Scratch-wound assay to determine the migratory capacity of DU145 and PC3 cells. (E, I) Transwell test to determine the quantity of DU145 and PC3 cells invading the lower chamber and assessing cell invasion ability. (F, J) Flow cytometry to detect apoptosis of DU145 and PC3 cells. (*P<0.05)

Fig. 5: PPLN reduced the malignant phenotype and caused apoptosis in prostate cancer cells by controlling the miR-3614-5p/SLC4A4 axis

and targets and could play an important role in controlling disease progression, reducing adverse effects, improving patients' quality of life, and extending survival time (Luo *et al*., 2019; Zhang *et al*., 2021). Many traditional Chinese remedies and their components have effects on prostate cancer through miRNA. For example, "Zhoushi Qiling decoction" increases apoptosis in prostate cancer cells by up-regulating miR-143 and decreases their resistance to docetaxel and glycolysis by up-regulating miR1271-5p (Cao *et al*., 2021a; Cao *et al*., 2021b). Icariin (ICA) and curcumin synergistically control the miR-7-mediated mTOR pathway in prostate cancer cells, resulting in autophagy and iron death (Xu *et al*., 2023). *Astragalus* polysaccharides suppressed prostate cancer carcinogenesis and lipid metabolism by inhibiting SIRT1 expression via miR-138-5p upregulation (Guo *et al*., 2020).

In the present investigation, 100 nM PPLN dramatically suppressed the proliferation, migration, and invasion behaviors of prostate cancer cells while increasing apoptosis, which was linked with decreased miR-3614-5p expression. MiR-3614-5p is down-regulated in a range of human malignancies, which contributes to the advancement of cancer. MiR-3614-5p expression is reduced in breast cancer cells while cadmium-induced cell proliferation and metastasis are increased via the modulation of TXNRD1 expression (Yue *et al*., 2022).

Overexpression of miR-3614-5p reversed the circ_0038985-induced enhancement of colorectal cancer cells' motility and invasion (Yao *et al*., 2023). LOXL1-AS1 targets and suppresses miR-3614-5p, resulting in overexpression of the downstream gene *YY1*. This increases proliferation, migration, and invasion and suppresses apoptosis in hepatocellular carcinoma cells,

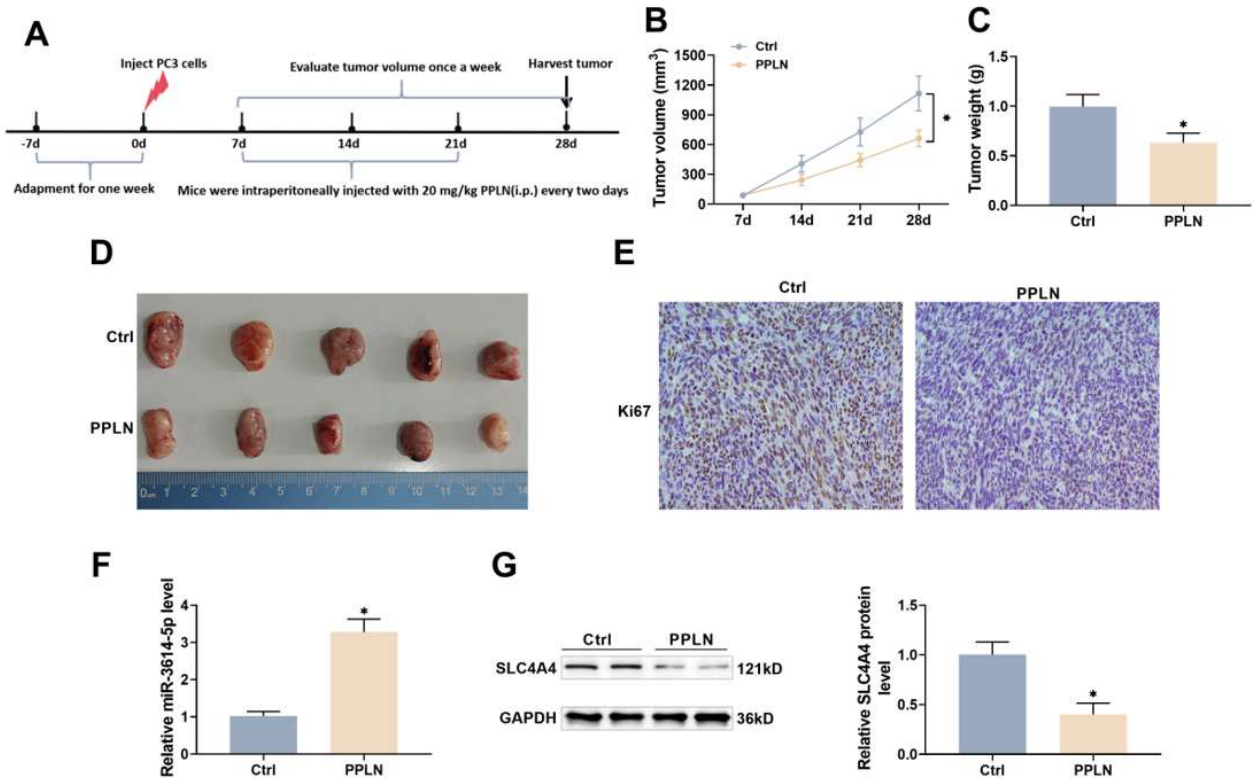

(A) Flowchart of subcutaneous tumor-graft model in nude mice. PC3 cells were injected subcutaneously. PPLN injection (20 mg/kg) was performed on day 7 following modeling once every 2 days for a total of 7 times. (B) Tumor volume. (C) Tumor weight. (D) Mice were sacrificed on day 28, and tumors were isolated and photographed. (E) Immunohistochemical detection of Ki67 expression in tumor tissues. (F) qRT-PCR for miR-3614-5p expression in tumor tissues. (G) Western blot for detecting SLC4A4 protein expression in tumor tissues. **P*<0.05

Fig. 6: PPLN inhibited tumor development.

which was efficiently reversed by inhibiting *YY1*expression (Feng *et al*., 2021).

Xie *et al*. (2022) discovered that overexpression of miR-3614-5p decreased Mcl-1 levels while increasing the synthesis of Mcl-1-associated pro-apoptotic proteins caspase-3 and PARP, which promoted apoptosis of prostate cancer cells. Using qRT-PCR, we found that the level of miR-3614-5p in prostate cancer cell lines DU145 and PC3 was lower than that in RWPE1 cells, which was consistent with the findings of Xie *et al*. PPLN treatment dramatically increased miR-3614-5p expression in prostate cancer cells, which inhibited cell proliferation, migration, and invasion while promoting apoptosis. When miR-3614-5p expression was low, PPLN's inhibitory impact on the malignancy of prostate cancer cells was reversed. This demonstrated that PPLN reduced the malignant advancement of prostate cancer cells by modulating miR-3614-5p levels.

Liu *et al*. (2022b) found that SLC4A4 was up-regulated in prostate cancer and acts as a tumor-promoting gene, which matches our results. In this investigation, SLC4A4 overexpression weakened the suppressive effect of miR-3614-5p overexpression on the proliferation, migration, and invasion behavior of prostate cancer cells while inhibiting apoptosis. SLC4A4 overexpression reduced the inhibitory impact of at transfected miR-3614-5p inhibitor on PPLN activity, which increased the effects of PPLN.

Notably, SLC4A4 has different roles in different types of cancer. Knockdown of SLC4A4 improves T-cell-mediated immune responses and disrupts macrophage-mediated immunosuppression, which inhibits the malignant progression of pancreatic cancer in mice (Cappellesso *et al*., 2022). A recent study showed that the expression level of SLC4A4 in colon cancer tissues was significantly lower than that in normal tissues, and the low expression positively correlated with poor prognosis (Yu *et al*., 2024). Future studies should elucidate the effects of the aberrant expression of SLC4A4 on different types of cancers and the specific mechanism of action.

The volume and weight measurements of the mouse tumors revealed that PPLN treatment successfully inhibited tumor growth. Ki67 expression was considerably lower in tumor tissues in the PPLN group than the control group, indicating growth inhibition of the prostate cancer cells. Ki67 expression is linked with poor prognosis in individuals with prostate cancer (Lotan *et al*., 2020), implying that PPLN could help to improve the prognosis.

PPLN limited the expression of SLC4A4 by up-regulating miR-3614-5p both *in vivo* and *in vitro*, thereby exerting an anti-development effect on prostate cancer. However, targeting a single miRNA often does not yield a complete therapeutic effect due to redundancy in cellular pathways and the complexity of the mechanisms of cancer progression. Additionally, overexpression of miR-3614-5p alone may not replicate the full biological impact of PPLN. Future studies should be done to further elucidate the effects of PPLN on miRNA networks in cancer and the regulatory mechanisms involved.

CONCLUSION

In summary, we have systematically examined the anti-tumor effects of PPLN on prostate cancer, the molecular mechanisms involved, and the targeting link between miR-3614-5p and SLC4A4. The findings expand on the biomarkers and therapeutic targets for prostate cancer, present data for the development of molecularly targeted medications for PPLN, and provide ideas for the improvement of therapeutic strategies. The study validated PPLN's effectiveness, although it is unclear how it interacts with other medications or whether other dose forms influence would the experimental outcomes. In the future, PPLN could be combined with other medications to investigate the potential synergistic effects of diverse drugs and the essential drug components using mass spectrometry, pharmacokinetics and other methods. In addition, clinical trials should be done to investigate the efficacy and safety of PPLN medicines in patients with varying features, as well as to establish precise therapy regimens to improve prognoses.

Conflict of interest

The authors report no conflict of interest.

REFERENCES

Bae ES, Byun WS, Ock CW, Kim WK, Park HJ and Lee SK (2023). Periplocin exerts antitumor activity by regulating nrf2-mediated signaling pathway in gemcitabine-resistant pancreatic cancer cells. *Biomed Pharmacother.,* **157**: 114039.

Bloise E, Braca A, De Tommasi N and Belisario MA (2009). Pro-apoptotic and cytostatic activity of naturally occurring cardenolides. *Cancer Chemother Pharmacol.,* **64**: 793-802.

Cao H, Wang D, Gao R, Chen L, Feng Y and Gao D (2021a). Zhoushi qiling decoction induces apoptosis of human prostate cancer cells via mir-143/bcl-2 axis. *Aging (Albany Ny),* **13**: 17202-17210.

Cao H, Wang D, Sun P, Chen L, Feng Y and Gao R (2021b). Zhoushi qi ling decoction represses docetaxel resistance and glycolysis of castration-resistant prostate cancer via regulation of Snhg10/Mir-1271-5p/Trim66 Axis. *Aging (Albany Ny),* **13**: 23096-23107.

Cappellesso F, Orban MP, Shirgaonkar N, Berardi E, Serneels J, Neveu MA, Di Molfetta D, Piccapane F, Caroppo R, Debellis L, Ostyn T, Joudiou N, Mignion L, Richiardone E, Jordan BF, Gallez B, Corbet C, Roskams T, Dasgupta R, Tejpar S, Di Matteo M, Taverna D, Reshkin SJ, Topal B, Virga F and Mazzone M (2022). Targeting the bicarbonate transporter slc4a4 overcomes immunosuppression and immunotherapy resistance in pancreatic cancer. *Nat Cancer,* **3**: 1464-1483.

Feng Z, Ye Z, Xie J, Chen W, Li W and Xing C (2021). Study on the mechanism of loxl1-as1/mir-3614-5p/yy1 signal axis in the malignant phenotype regulation of hepatocellular carcinoma. *Biol Direct,* **16**: 24.

Fu XP, Ji CY, Tang WQ, Yu TT and Luo L (2024). Long Non-Coding Rna Loxl1-As1: A potential biomarker and therapeutic target in human malignant tumors. *Clin. Exp. Med.,* **24**: 93.

Gandaglia G, Karakiewicz PI, Briganti A, Passoni NM, Schiffmann J, Trudeau V, Graefen M, Montorsi F & Sun M (2015). Impact of the site of metastases on survival in patients with metastatic prostate cancer. *Eur. Urol.,* **68**: 325-34.

Guccini I, Revandkar A, D'ambrosio M, Colucci M, Pasquini E, Mosole S, Troiani M, Brina D, Sheibani-Tezerji R, Elia AR, Rinaldi A, Pernigoni N, Ruschoff J H, Dettwiler S, De Marzo AM, Antonarakis ES, Borrelli C, Moor AE, Garcia-Escudero R, Alajati A, Attanasio G, Losa M, Moch H, Wild P, Egger G & Alimonti A (2021). Senescence reprogramming by timp1 deficiency promotes prostate cancer metastasis. *Cancer Cell,* **39**: 68-82 E9.

Guo S, Ma B, Jiang X, Li X and Jia Y (2020). Astragalus polysaccharides inhibits tumorigenesis and lipid metabolism through mir-138-5p/sirt1/srebp1 pathway in prostate cancer. *Front Pharmacol.,* **11**: 598.

Han L, Sun Y, Lu C, Ma C, Shi J and Sun D (2021). Mir-3614-5p is a potential novel biomarker for colorectal cancer. *Front Genet,* **12**: 666833.

Hao J, Chang L, Wang D, Ji C, Zhang S, Hou Y and Wu Y (2023). Periplocin alleviates cardiac remodeling in doca-salt-induced heart failure rats. *J Cardiovasc Transl Res.,* **16**: 127-140.

Hsieh YH, Yu FJ, Nassef Y, Liu CJ, Chen YS, Lin CY, Feng JL and Wu MH (2022). Targeting of mcl-1 expression by mirna-3614-5p promotes cell apoptosis of human prostate cancer cells. *Int. J. Mol. Sci.,* **23**: 4194.

Hussen BM, Hidayat HJ, Salihi A, Sabir DK, Taheri M and Ghafouri-Fard S (2021). Microrna: A signature for cancer progression. *Biomed Pharmacother,* **138**: 111528.

Khanmi K, Ignacimuthu S and Paulraj MG (2015). Microrna In Prostate Cancer. *Clin Chim Acta,* **451**: 154-60.

Lacouture A, Lafront C, Peillex C, Pelletier M and Audet-Walsh E (2022). Impacts of endocrine-disrupting

chemicals on prostate function and cancer. *Environ Res.,* **204**: 112085.

Li F, Yang H, Kong T, Chen S, Li P, Chen L, Cheng J, Cui G and Zhang G (2020). Pgam1, regulated by mir-3614-5p, functions as an oncogene by activating transforming growth factor-beta (tgf-beta) signaling in the progression of non-small cell lung carcinoma. *Cell Death Dis.,* **11**: 710.

Li Y, Li J, Zhou K, He J, Cao J, An M and Chang YX (2016). A review on phytochemistry and pharmacology of cortex periplocae. *Molecules,* **21**: 1702.

Lin JP, Huang MH, Sun ZT, Chen L, Lei YH, Huang Y Q, Qi M, Fan SR, Chen, SG, Chung CW, Chan MC, Liu JS, Hu M, Chen MF, Ye WC, Chen YY and Deng LJ (2023). Periplocin inhibits hepatocellular carcinoma progression and reduces the recruitment of mdscs through akt/nf-kappab pathway. *Life Sci.,* **324**: 121715.

Liu J, Dong L, Zhu Y, Dong B, Sha J, Zhu HH, Pan J and Xue W (2022a). Prostate Cancer Treatment - China's Perspective. *Cancer Lett.,* **550**: 215927.

Liu Z, Wang Q, Zhai G, Ke S, Yu X and Guo J (2022b). Slc4a4 promotes prostate cancer progression *in vivo* and *in vitro* via akt-mediated signalling pathway. *Cancer Cell Int.,* **22**: 127.

Lotan TL, Tomlins SA, Bismar TA, Van Der Kwast TH, Grignon D, Egevad L, Kristiansen G, Pritchard CC, Rubin MA and Bubendorf L (2020). Report from the International Society of Urological Pathology (ISUP) consultation conference on molecular pathology of urogenital cancers. I. molecular biomarkers in prostate cancer. *Am. J. Surg Pathol.,* **44**: E15-E29.

Luo H, Vong CT, Chen H, Gao Y, Lyu P, Qiu L, Zhao M, Liu Q, Cheng Z, Zou J, Yao P, Gao C, Wei J, Ung CO L, Wang S, Zhong Z and Wang Y (2019). Naturally occurring anti-cancer compounds: Shining from chinese herbal medicine. *Chin Med.,* **14**: 48.

Markowski MC and Carducci MA (2017). Early use of chemotherapy in metastatic prostate cancer. *Cancer Treat Rev.,* **55**: 218-224.

Shang J, Wang Z, Chen W, Yang Z, Zheng L, Wang S and Li S (2019). Pseudogene chiap2 inhibits proliferation and invasion of lung adenocarcinoma cells by means of the wnt pathway. *J Cell Physiol,* **234**: 13735-13746.

Sharma, K. K., Gupta, S. and Bisen, P. S. (2025). Enhancing Gastrointestinal (GI) Cancer therapies with ganoderma lucidum: A review of mechanisms and efficacy. *J Can Biomol Therap*, **2**: 15-44.

Sung H, Ferlay J, Siegel RL, Laversanne M, Soerjomataram I, Jemal A and Bray F (2021). Global cancer statistics 2020: Globocan estimates of incidence and mortality worldwide for 36 cancers in 185 countries. *Ca Cancer J Clin,* **71**: 209-249.

Wang G, Zhao D, Spring DJ and Depinho RA (2018). Genetics and biology of prostate cancer. *Genes Dev,* **32**: 1105-1140.

Wang K, Fu S, Dong L, Zhang D, Wang M, Wu X, Shen E, Luo L, Li C, Nice EC, Huang C and Zou B (2023). Periplocin suppresses the growth of colorectal cancer cells by triggering Lgals3 (Galectin 3)-Mediated Lysophagy. *Autophagy,* **19**: 3132-3150.

Wang Z, Tong D, Han C, Zhao Z, Wang X, Jiang T, Li Q, Liu S, Chen L, Chen Y, Li A and Huang C (2019). Blockade of Mir-3614 maturation by Igf2bp3 Increases Trim25 expression and promotes breast cancer cell proliferation. *Ebiomedicine.,* **41**: 357-369.

Xia C, Dong X, Li H, Cao M, Sun D, He S, Yang F, Yan X, Zhang S, Li N and Chen W (2022). Cancer statistics in china and United States, 2022: Profiles, Trends, and determinants. *Chin Med J (Engl),* **135**: 584-590.

Xie G, Sun L, Li Y, Chen B and Wang C 2021. Periplocin inhibits the growth of pancreatic cancer by inducing apoptosis via Ampk-Mtor signaling. *Cancer Med,* **10**: 325-336.

Xu W, Ding J, Li B, Sun T, You X, He Q and Sheng W (2023). Effects of icariin and curcumol on autophagy, ferroptosis and lipid metabolism based on mir-7/m-tor/srebp1 pathway on prostate cancer. *Biofactors.,* **49**: 438-456.

Yao H, Zhou X, Zhou A, Chen J, Chen G, Shi X, Shi B, Tai Q, Mi X, Zhou G, Wang S, Sun J, Yang X, Yang Y, Cao H, Zhou D, Sun L., Yao Y and He S (2023). Rfc5, regulated by Circ_0038985/Mir-3614-5p, Functions as an oncogene in the progression of colorectal cancer. *Mol. Carcinog.,* **62**: 771-785.

Yu C, Li H, Zhang C, Tang Y, Huang Y, Lu H, Jin K, Zhou J and Yang J (2024). Solute carrier family 4 member 4 (slc4a4) is associated with cell proliferation, migration and immune cell infiltration in colon cancer. *Discov Oncol.,* **15**: 597.

Yue Y, Tan M, Luo Y, Deng P, Wang H, Li J, Hao R, Tian L, Xie J, Chen M, Yu Z, Zhou Z and Pi H (2022). Mir-3614-5p downregulation promotes cadmium-induced breast cancer cell proliferation and metastasis by targeting txnrd1. *Ecotoxicol Environ Saf,* **247**: 114270.

Zhang X, Qiu H, Li C, Cai P and Qi F (2021). The positive role of traditional chinese medicine as an adjunctive therapy for cancer. *Biosci Trends,* **15**: 283-298.

Zhou J, Jiang YY, Chen H, Wu YC and Zhang L (2020). Tanshinone I attenuates the malignant biological properties of ovarian cancer by inducing apoptosis and autophagy via the inactivation of pi3k/akt/mtor pathway. *Cell Prolif.,* **53**: E12739.